Recent Advances in Polyphenol Research

Volume 7

Edited By
Jess Reed,
Victor de Freitas,
and Stéphane Quideau

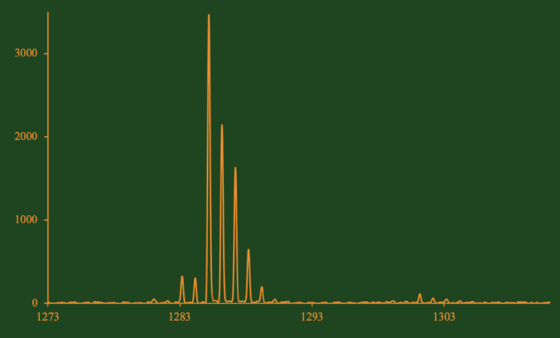

WILEY Blackwell

Recent Advances in Polyphenol Research

Recent Advances in Polyphenol Research

A series for researchers and graduate students whose work is related to plant phenolics and polyphenols, as well as for individuals representing governments and industries with interest in this field. Each volume in this biennial series focuses on several important research topics in plant phenols and polyphenols, including chemistry, biosynthesis, metabolic engineering, ecology, physiology, food, nutrition, and health.

Recent Advances in Polyphenol Research

Volume 7

Edited by

Jess Dreher Reed
Professor, Nutrition and Phytochemistry
Department of Animal Sciences,
College of Agricultural and Life Sciences
University of Wisconsin–Madison, Madison, USA
Complete Phytochemical Solutions LLC,
Cambridge, Wisconsin, USA

Victor Armando Pereira de Freitas
Professor, Food Chemistry
Chemistry and Biochemistry Department, Faculty of Sciences
University of Porto, Porto, Portugal

Stéphane Quideau
Professor, Organic and Bio-organic Chemistry
Institut des Sciences Moléculaires, CNRS-UMR 5255
University of Bordeaux, Talence, France
& Institut Universitaire de France, Paris, France

WILEY Blackwell

This edition first published 2021

Registered Office(s)
John Wiley & Sons, Inc., 111 River Street, Hoboken, NJ 07030, USA
John Wiley & Sons Ltd, The Atrium, Southern Gate, Chichester, West Sussex, PO19 8SQ, UK

Editorial Office
The Atrium, Southern Gate, Chichester, West Sussex, PO19 8SQ, UK

For details of our global editorial offices, customer services, and more information about Wiley products visit us at www.wiley.com.

Wiley also publishes its books in a variety of electronic formats and by print-on-demand. Some content that appears in standard print versions of this book may not be available in other formats.

Library of Congress Cataloging-in-Publication data applied for

ISBN: 9781119545927
ISSN: 2474-7696

Cover Design: Wiley
Cover Images: © Reed Research Group

Set in 9.5/12.5pt STIXTwoText by SPi Global, Pondicherry, India

10 9 8 7 6 5 4 3 2 1

Contents

Contributors

Nick W. Albert
Plant & Food Research, Palmerston North, New Zealand

C. Peter Constabel
Centre for Forest Biology and Biology Department, University of Victoria, Victoria, Canada

Kevin M. Davies
Plant & Food Research, Palmerston North, New Zealand

Kriya Dunlap
Department of Biochemistry, University of Alaska Fairbanks, Fairbanks, USA

Daniel Esquivel-Alvarado
Department of Animal Sciences, University of Wisconsin–Madison, Madison, USA

Ana Gutiérrez
Instituto de Recursos Naturales y Agrobiología de Sevilla (IRNAS), CSIC, Seville, Spain

Rubina Jibran
Plant & Food Research, Palmerston North, New Zealand

James A. Kennedy
Functional Phenolics, LLC, Corvallis, USA

Christian G. Krueger
Complete Phytochemical Solutions LLC, Cambridge, Wisconsin, USA
Department of Animal Sciences, University of Wisconsin–Madison, Madison, USA

Hoon Kim
Department of Energy Great Lakes Bioenergy Research Center, Wisconsin Energy Institute
University of Wisconsin–Madison, Madison, USA

Wu Lan
Department of Biological System Engineering University of Wisconsin–Madison, Madison, USA & Department of Energy Great Lakes Bioenergy Research Center, Wisconsin Energy Institute
University of Wisconsin–Madison, Madison, USA

Mary Ann Lila
Department of Food Bioprocessing and Nutrition Sciences, Plants for Human Health Institute, North Carolina State University, Kannapolis, USA

Richard L. Lindroth
Department of Entomology, University of Wisconsin–Madison, Madison, USA

Dawei Ma
Centre for Forest Biology and Biology Department, University of Victoria, Victoria, Canada

Johan Mendoza
Department of Chemistry, Nova School of Science and Technology, Caparica Portugal

Irene Mueller-Harvey
School of Agriculture, Policy and Development, University of Reading, Reading, UK

Ken Ohmori
Department of Chemistry, Tokyo Institute of Technology, Tokyo, Japan

Marisa S. Otegui
Department of Botany, University of Wisconsin–Madison, Madison, USA

Fernando Pina
Department of Chemistry, Nova School of Science and Technology, Caparica, Portugal

John Ralph
Department of Energy Great Lakes Bioenergy Research Center, Wisconsin Energy Institute, University of Wisconsin–Madison, Madison, USA & Department of Biochemistry, University of Wisconsin–Madison, Madison, USA

Jess Dreher Reed
Department of Animal Sciences, University of Wisconsin–Madison, Madison, USA
Complete Phytochemical Solutions LLC, Cambridge, Wisconsin, USA

Jorge Rencoret
Instituto de Recursos Naturales y Agrobiología de Sevilla (IRNAS), CSIC, Seville, Spain

José C. del Río
Instituto de Recursos Naturales y Agrobiología de Sevilla (IRNAS), CSIC, Seville, Spain

Kennedy F. Rubert-Nason
Division of Natural and Behavioral Sciences University of Maine–Fort Kent, Fort Kent, USA

Kathy E. Schwinn
Plant & Food Research, Palmerston North, New Zealand

Keisuke Suzuki
Department of Chemistry, Tokyo Institute of Technology, Tokyo, Japan

Wayne E. Zeller
ARS-USDA, U.S. Dairy Forage Research Center, Madison, USA

Yanfei Zhou
Plant & Food Research, Palmerston North, New Zealand

Preface

Every two years, Groupe Polyphénols (GP) hosts the International Conference on Polyphenols (ICP). The XXIX ICP was the first one to be held in the United States in Madison, Wisconsin, on the campus of the University of Wisconsin–Madison (UW–Madison), from July 16 to 20, 2018. Groupe Polyphénols also hosted the 9th Tannin Conference (TC) concurrently with the XXIX ICP. Groupe Polyphénols was founded in 1972 and is the world's premier society of scientists in the fields of polyphenol chemistry, synthesis, bioactivity, nutrition, industrial applications, and ecology.

Madison is Wisconsin's state capital (the capitol building is shown on the front cover) and one of the nicest cities in the great lakes region. UW–Madison is a top ranked University (25th worldwide and 19th in the USA) and has a lovely campus with miles of lakefront and beautiful scenery adjacent to the state capitol. This venue for the XXIX ICP and 9th TC was fitting because Wisconsin's cranberry industry provides 60 percent of the world's supply of cranberries and is the state's largest fruit industry. The cranberry industry is also strongly dependent on the polyphenolic composition of the fruit. Cranberries are harvested in the fall after they turn from yellow-green to bright red, as shown on the front cover. The fruits are harvested by flooding the marsh (also called cranberry bogs). After removing the fruits from the vine, they float to the surface and are corralled with a floating boom and conveyed into trucks (as depicted on the front cover). The fruits are either transferred to a packaging facility for the fresh fruit market or to a frozen storage facility for subsequent processing into juice or sweetened dried cranberries (SDC). In both cases the bright red color of the fruit is a critical component of processing because the fruit is sorted based on color before packaging as fresh fruit or processing for juice and SDC (a processing line after sorting is also shown on the front cover). The color is a function of six anthocyanins, cyanidin 3-O-galactoside, cyanidin 3-O-glucoside, cyanidin 3-O-arabinoside, peonidin 3-O-galactoside, peonidin 3-O-glucoside, and peonidin 3-O-arabinoside. In addition to the anthocyanins, cranberries contain a large diversity of other monomeric polyphenols, especially flavonol glycosides, and contain simple phenols such as hydroxycinnamic acids and hydroxybenzoic acids. Cranberries also contain proanthocyanidins, which are just as important to the economic value of the fruit as the anthocyanins. The importance of proanthocyanidins to the cranberry market is a result of pioneering research from the late 1990s in which "A-type" interflavan bonds were discovered to be the structural feature of cranberry proanthocyanidins that is associated with the prevention of adherence of P-fimbriated *E. coli* to uroepithelial cells, the putative mechanism in the prevention of urinary tract

infections. Proanthocyanidin content is now used to market cranberry products (including juice, sweetened dried cranberries, and dietary supplements) and consumers widely recognize cranberries as healthy. Therefore, all of the subjects that were discussed at the XXIX ICP and 9th TC and the chapters of this volume of *Recent Advances in Polyphenol Research* are of direct importance to Wisconsin's cranberry industry. The role of polyphenols in this industry is an excellent example of the importance of polyphenol research in general.

The XXIX ICP and 9th TC were attended by 189 registrants from 23 countries, with 62 invited and contributed presentations and 104 posters. This seventh edition of *Recent Advances in Polyphenol Research* presents 11 chapters that represent the work of the invited speakers at the XXIX ICP and 9th TC and reflect the depth of science in this important field of natural product chemistry. The conference included sessions on the chemistry and physical chemistry of polyphenols; synthesis, genetics and metabolic engineering of polyphenols; the effects of polyphenols on the nutrition and health of humans and animals; the role of polyphenols in plants and ecosystems; applied research on polyphenols; and a special session devoted to the 9th Tannin Conference.

We owe a special thanks to Hannah Scott and Laura Richards from the Campus Events Services, UW–Madison, for their professional and excellent organization of the conference. Finally, we thank all of the participants, some who traveled a great distance to come to Madison, for making the conference a very enjoyable event and a wonderful learning experience.

Jess Dreher Reed
Victor Armando Pereira de Freitas
Stéphane Quideau

Acknowledgements

The editors wish to thank all of the members of the Groupe Polyphénols Board Committee (2016–2018 & 2018–2020) for their guidance and assistance throughout this project.

Groupe Polyphénols Board 2016–2018 & 2018–2020

Dr. Denis Barron
Dr. Luc Bidel
Dr. Catherine Chèze
Dr. Peter Constabel
Prof. Olivier Dangles
Dr. Kevin Davies
Prof. M Teresa Escribano
Prof. Victor Armando Pereira de Freitas
Prof. Kazuhiko Fukushima
Dr. David Gang
Dr. Sylvain Guyot
Prof. Ann E. Hagerman
Prof. Heidi Halbwirth
Prof. Amy Howell
Dr. Stefan Martens
Dr. Fulvio Mattivi
Dr. Irene Mueller-Harvey
Prof. Stéphane Quideau
Prof. Jess Dreher Reed
Dr. Erika Salas
Prof. Juha-Pekka Salminen
Prof. Kathy Schwinn
Dr. David Vauzour
Prof. Kristiina Wähälä

1

Achieving Complexity at the Bottom Through the Flavylium Cation-Based Multistate

A Comprehensive Kinetic and Thermodynamic Study

Johan Mendoza and Fernando Pina

Department of Chemistry, Nova School of Science and Technology, Caparica, Portugal

1.1 Introduction

Complexity is ubiquitous in biological systems. The main strategy to study complexity has been carried out using a top-down approach. Though the top-down approach the simpler components of the complex systems are identified, and whenever possible, up to the molecular level. In contrast, supramolecular chemistry, a concept well established and recognized after the 1987 Nobel Prize awarded to Donald J. Cram, Jean-Marie Lehn, and Charles J. Pedersen, is a bottom-up approach (Figure 1.1). Supramolecular chemistry studies how molecules interact to form higher-dimension entities and tends to fill the gap between "classical chemistry" and biology (Lehn, 1995).

A beautiful example of supramolecular chemistry is the structure of the metalloanthocyanin that gives color to *Commelina communis* (Kondo et al. 1992; Yoshida et al. 2009). An anthocyanin, a flavone, and a metal ion in a ratio 6:6:2 are organized into two parallel plans, each one containing three anthocyanins, three flavones, and one metal ion that organizes the space Figure 1.1.

There is an alternative to achieve complexity that we coin *metamorphosis* (Petrov et al. 2012). When a molecule (generator) is able to be transformed into other molecules by means of successive conversions and as a response to external stimuli, new molecules are formed. The complexity results from the number of the species and everything takes place at the bottom.

The pH-dependent multistate of species of anthocyanins and related compounds is a paradigm of the metamorphosis concept; see Scheme 1.1.

1.2 Flavylium Cation as a Metamorphosis Generator

The flavylium cation, $\mathbf{AH^+}$, is the most stable species at very low pH values, in anthocyanins generally for pH<1. The system is conveniently studied by *direct pH jumps* when base is added to the flavylium cation, and *reverse pH jumps*, defined as addition of acid to

Recent Advances in Polyphenol Research, Volume 7, First Edition. Edited by Jess Dreher Reed, Victor Armando Pereira de Freitas, and Stéphane Quideau.

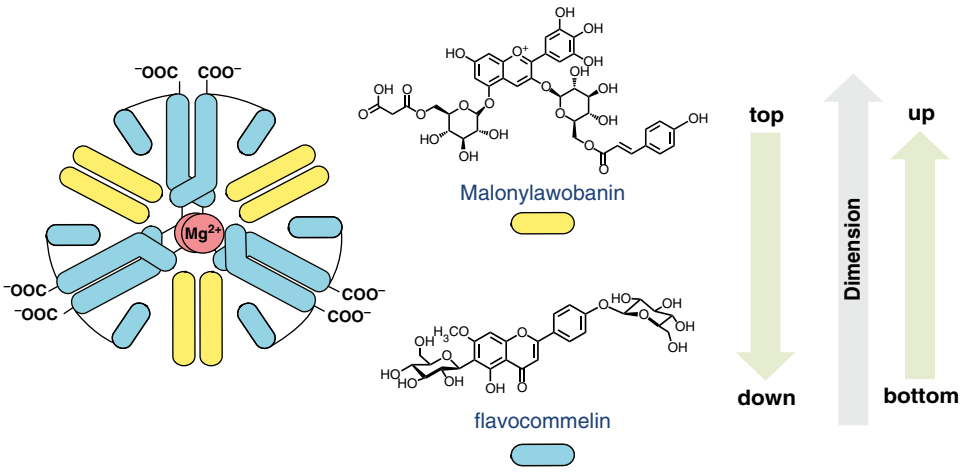

Figure 1.1 Sketch of the metalloanthocyanin responsible for the color in *Cummelina communis*. The building blocks self-associate to create the supramolecule in a bottom-up approach. *Source:* Courtesy of Prof. Kumi Yoshida.

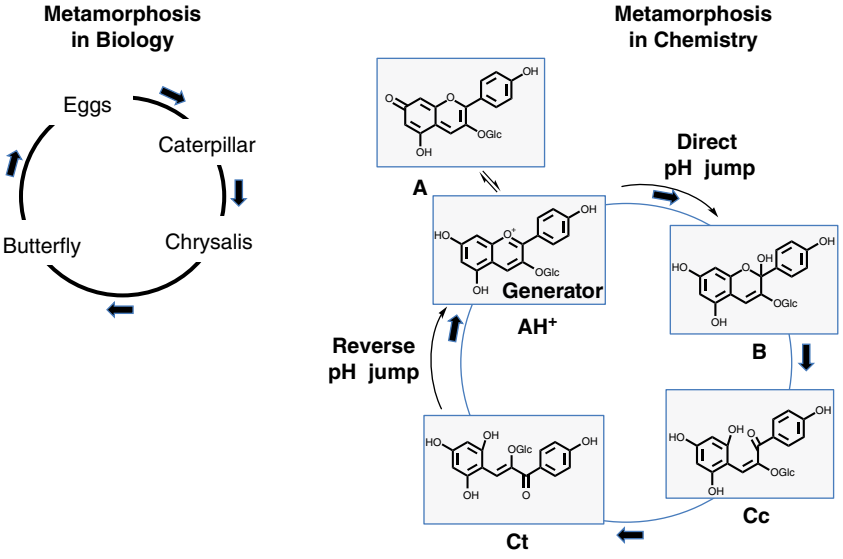

Scheme 1.1 The metamorphosis concept in biology and in chemistry applied to anthocyanins and related compounds in acidic medium. *Source:* Reproduced from Mendoza et al. (2018), with permission.

equilibrated solutions at higher pH values. After a direct pH jump to moderately acidic pHs, the flavylium cation equilibrates in microseconds with quinoidal base, **A** eq. (1). The next step is the formation of the hemiketal, **B**, through the hydration of $\mathbf{AH}^+$ (min) eq. (2), followed by the ring opening to form *cis*-chalcone, **Cc**, (ms) eq. (3). The fact that the quinoidal base does not open in acidic medium is a breakthrough discovery (Brouillard and Dubois 1977) crucial for the comprehension of anthocyanins and related

compounds systems. The **Cc** isomerization to *trans*-chalcone, **Ct**, in anthocyanins takes place in several hours eq. (4). When the system is equilibrated in moderately acidic pH values, a reverse pH jumps restores the flavylium cation. The following set of equilibrium reactions accounts for the system:

$$\mathbf{AH}^+ + H_2O \underset{k_{-a}}{\overset{k_a}{\rightleftarrows}} \mathbf{A} + H_3O^+ \qquad K_a \quad \text{proton transfer} \qquad (1)$$

$$\mathbf{AH}^+ + 2H_2O \underset{k_{-h}}{\overset{k_h}{\rightleftarrows}} \mathbf{B} + H_3O^+ \qquad K_h \quad \text{hydration} \qquad (2)$$

$$\mathbf{B} \underset{k_{-t}}{\overset{k_t}{\rightleftarrows}} \mathbf{Cc} \qquad K_t \quad \text{tautomerization} \qquad (3)$$

$$\mathbf{Cc} \underset{k_{-i}}{\overset{k_i}{\rightleftarrows}} \mathbf{Ct} \qquad K_i \quad \text{isomerization} \qquad (4)$$

A few years ago we introduced an energy level diagram that accounts for the thermodynamic of the anthocyanin system in acidic medium (Pina et al. 1997; Pina 2014a). This diagram can be straightforwardly constructed provided that the equilibrium constants, eq. (1) to eq. (4), of the system have been determined, see Scheme 1.2.

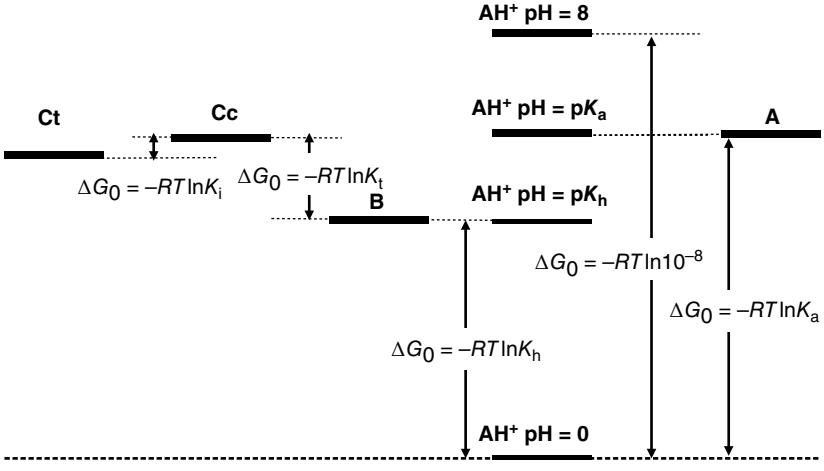

Scheme 1.2 Energy level diagram for anthocyanins and related compounds in acidic medium. *Source:* Adapted from Pina 2014a. © 2014 John Wiley & Sons.

1.3 Extending the Multistate of Anthocyanins and Related Compounds to the Basic Region

In many flavylium derivatives from natural or synthetic origin, including anthocyanins, it is indispensable to extend the multistate study to basic medium.

In order to account for these new species, eight equilibrium equations should be added to eq. (1) through eq. (4).

For the formation of the mono-anionic species[1]

$$\mathbf{A} + H_2O \rightleftharpoons \mathbf{A}^- + H_3O^+ \qquad K_{A/A^-} \quad \text{proton transfer} \tag{5}$$

$$\mathbf{B} + H_2O \rightleftharpoons \mathbf{B}^- + H_3O^+ \qquad K_{B/B^-} \quad \text{proton transfer} \tag{6}$$

$$\mathbf{Cc} + H_2O \rightleftharpoons \mathbf{Cc}^- + H_3O^+ \qquad K_{Cc/Cc^-} \quad \text{proton transfer} \tag{7}$$

$$\mathbf{Ct} + H_2O \rightleftharpoons \mathbf{Ct}^- + H_3O^+ \qquad K_{Ct/Ct^-} \quad \text{proton transfer} \tag{8}$$

And for the formation of the di-anionic species

$$\mathbf{A}^- + H_2O \rightleftharpoons \mathbf{A}^{2-} + H_3O^+ \qquad K_{A^-/A^{2-}} \quad \text{proton transfer} \tag{9}$$

$$\mathbf{B}^- + H_2O \rightleftharpoons \mathbf{B}^{2-} + H_3O^+ \qquad K_{B^-/B^{2-}} \quad \text{proton transfer} \tag{10}$$

$$\mathbf{Cc}^- + H_2O \rightleftharpoons \mathbf{Cc}^{2-} + H_3O^+ \qquad K_{Cc^-/Cc^{2-}} \quad \text{proton transfer} \tag{11}$$

$$\mathbf{Ct}^- + H_2O \rightleftharpoons \mathbf{Ct}^{2-} + H_3O^+ \qquad K_{Ct^-/Ct^{2-}} \quad \text{proton transfer} \tag{12}$$

The system can be generalized for higher charged anionic species.

In spite of the complexity of this system, the set of eqs. 1 through 12 can be simplified considering a triprotic acid, eq. (13) through eq. (15), with constants K'_a, eq. (19) K''_a, eq. (20), and K'''_a, eq. (21). The complete mathematical development of the system above was previously reported (supplementary information, Mendoza et al. 2019) and is straightforwardly obtained from a mass balance and representation of all species as a function of $\mathbf{AH}^+$.

$$\mathbf{AH}^+ + H_2O \rightleftharpoons \mathbf{CB} + H_3O^+ \qquad K'_a \tag{13}$$

$$\mathbf{CB} + H_2O \rightleftharpoons \mathbf{CB}^- + H_3O^+ \qquad K''_a \tag{14}$$

$$\mathbf{CB}^- + H_2O \rightleftharpoons \mathbf{CB}^{2-} + H_3O^+ \qquad K'''_a \tag{15}$$

Where

$$[\mathbf{CB}] = [\mathbf{A}] + [\mathbf{B}] + [\mathbf{Cc}] + [\mathbf{Ct}] \tag{16}$$

$$[\mathbf{CB}^-] = [\mathbf{A}^-] + [\mathbf{B}^-] + [\mathbf{Cc}^-] + [\mathbf{Ct}^-] \tag{17}$$

$$[\mathbf{CB}^{2-}] = [\mathbf{A}^{2-}] + [\mathbf{B}^{2-}] + [\mathbf{Cc}^{2-}] + [\mathbf{Ct}^{2-}] \tag{18}$$

and

$$K'_a = K_a + K_h + K_h K_t + K_h K_t K_i \tag{19}$$

$$K''_a = \frac{K_{A/A^-}K_a + K_{B/B^-}K_h + K_{Cc/Cc^-}K_h K_t + K_{Ct/Ct^-}K_h K_t K_i}{K'_a} \tag{20}$$

$$K'''_a = \frac{K_{A-/A2-}K_{A/A-}K_a + K_{B-/B2-}K_{B/B-}K_h + K_{Cc-/Cc2-}K_{Cc/Cc-}K_hK_t + K_{Ct-/Ct2-}K_{Ct/Ct-}K_hK_tK_i}{K'_aK''_a} \tag{21}$$

The mole fraction distribution X_R of all species can be expressed in terms of the 12 linearly independent constants reported in Scheme 1.3. Since the flavylium cation and the quinoidal bases are in very fast equilibrium (microseconds scale), it is convenient to consider them altogether. The same is valid for the other species related through the proton transfer reaction.

$$X_{AH+} + X_A + X_{A-} + X_{A2-} = \frac{\left[H^+\right]^3 + K_a\left[H^+\right]^2 + K_{A/A-}K_a\left[H^+\right] + K_{A-/A2-}K_{A/A-}K_a}{D} \tag{22}$$

where

$$D = \left[H^+\right]^3 + K'_a\left[H^+\right]^2 + K'_aK''_a\left[H^+\right] + K'_aK''_aK'''_a \tag{23}$$

$$X_B + X_{B-} + X_{B2-} = \frac{K_h\left[H^+\right]^2 + K_{B/B-}K_h\left[H^+\right] + K_{B-/B2-}K_{B/B-}K_h}{D} \tag{24}$$

$$X_{Cc} + X_{Cc-} + X_{Cc2-} = \frac{K_hK_t\left[H^+\right]^2 + K_{Cc/Cc-}K_hK_t\left[H^+\right] + K_{Cc-/Cc2-}K_{Cc/Cc-}K_hK_t}{D} \tag{25}$$

$$X_{Ct} + X_{Ct-} + X_{Ct2-} = \frac{K_hK_tK_i\left[H^+\right]^2 + K_{Ct/Ct-}K_hK_tK_i\left[H^+\right] + K_{Ct-/Ct2-}K_{Ct/Ct-}K_hK_tK_i}{D} \tag{26}$$

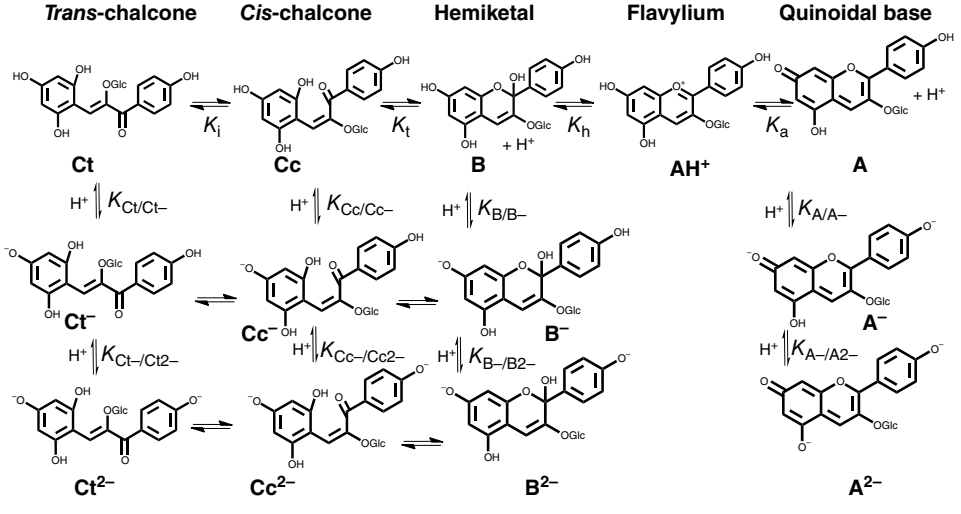

Scheme 1.3 Extension to the basic medium of Pelargonidin-3-glucoside.

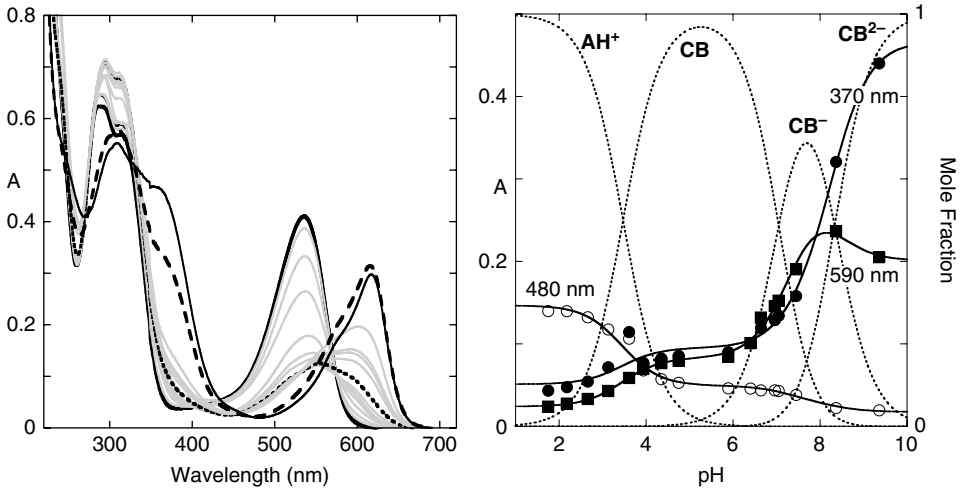

Figure 1.2 Absorption spectrum of heavenly blue anthocyanin, a peonidin derivative, black full line, flavylium cation; black pointed line, quinoidal base; black traced line, ionized quinoidal base. pK'_a=3.47; pK''_a=7.05; pK'''_a=8.30. *Source:* Mendoza et al. 2018.

Since the complex system shown in Scheme 1.3 behaves as a simple triprotic acid, the respective apparent equilibrium constants K'_a, K''_a, and K'''_a are experimentally obtained from the inflection points of the absorbance representation as a function of the pH. Consequently, the term ***D*** is a parameter obtained experimentally. In Figure 1.2 the example of the heavenly blue anthocyanin is shown (Mendoza et al. 2018).

The question now is to define the experimental strategy to calculate the equilibrium constants of the system.

1.3.1 Reverse pH Jumps from Pseudo-equilibrium Followed by Stopped Flow UV-visible Spectroscopy

Recently we have reported a new experimental procedure that allows the experimental determination of all equilibrium constants (as shown in Scheme 1.3) of the flavylium-based multistates including anthocyanins (Mendoza et al. 2019; Mendoza et al. 2018; Slavcheva et al. 2018). It is based on the reverse pH jumps defined above, followed by stopped flow. In Figure 1.3 the stopped flow traces of the model compound 4'-hydroxyflavylium are shown. The initial solutions should be equilibrated or pseudo-equilibrated. The reverse pH jumps consist of the addition of acid to make the solutions with pH=1, where flavylium cation is the sole species. In both cases of Figure 1.3 the initial absorbance is due to the quinoidal bases (independently on their protonation state) that give flavylium cation (absorption at 450 nm) during the mixing time of the stopped flow together with some flavylium cation present at the initial equilibrium (at lower pH values) prior to the jump; see also Scheme 1.3. This is the reason why the mole fraction distribution of the flavylium cation and quinoidal bases are

represented together in eq. (22). At the final very low pH jump (pH=1) the hydration reaction becomes faster than the tautomerization because it is directly proportional to the proton concentration (Pina 2014b). Therefore, the faster trace is due to the conversion of **B** into $\mathbf{AH^+}$. The slower trace is the formation of more flavylium cation from **Cc** via **B** (Scheme 1.4) (Mendoza et al. 2019).

In anthocyanins and most flavylium derivatives the *cis-trans* isomerization is much slower than the other kinetic processes. It is possible thus to define a transient state (pseudo-equilibrium) where the mole fraction of the *trans*-chalcones is very small. Consequently, it is more convenient to carry out the reverse pH jumps from

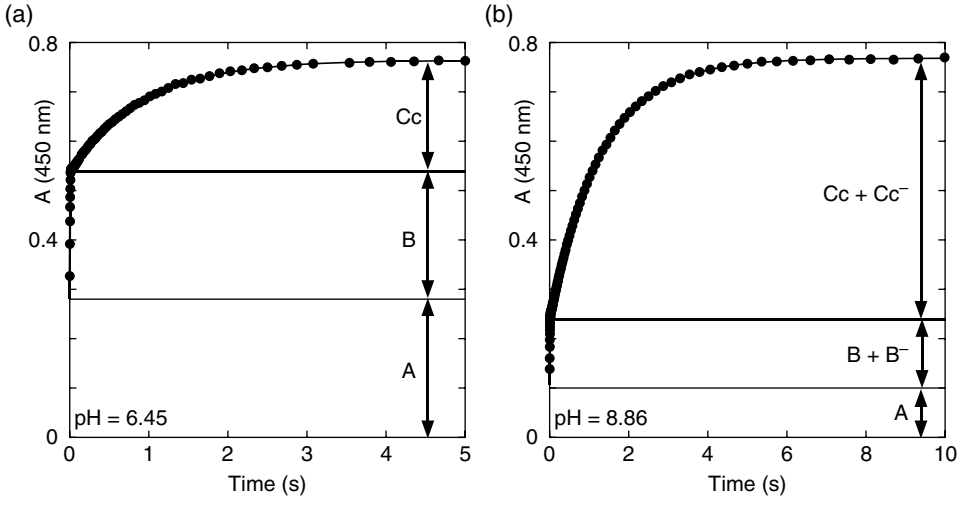

Figure 1.3 Stopped flow traces 4'-hydroxyflavylium (at pseudo-equilibrium, where no significant amounts of **Ct** were formed) after a reverse pH jump from pH=6.45 (a) and pH=8.9 (b) to the final pH=1.0.

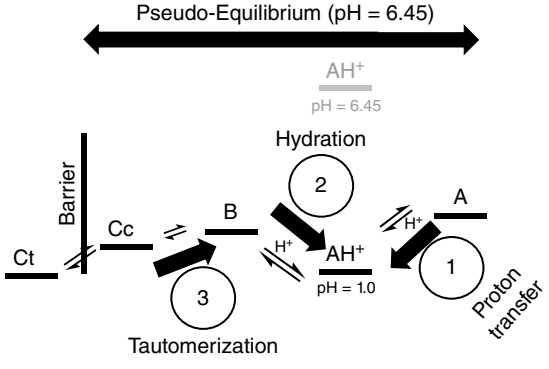

Scheme 1.4 Energy level diagram of the compound 4'-hydroxyflavylium and the kinetic processes after a reverse pH jump to pH≤1.

pseudo-equilibrium. Scheme 1.4 illustrates the question in acidic medium, but it is generalized to higher pH values. Even if some **Ct** is formed, the only drawback is the loss of sensitivity, because the kinetics of the **Ct** transformation in flavylium cation is much slower and is not detected in the stopped flow experiments. In conclusion, the data reported in Figure 1.3, extended to other pH values, allows the calculation of the mole fraction distribution of the species **A**, **B**, and **Cc** as well as the respective anionic forms.

The mole fraction distribution of these species can be represented as a function of the initial pH of the reverse pH jump (Figure 1.4).

The fitting of Figure 1.4 was carried out by considering for $\mathbf{AH^+}$, $\mathbf{CB^{\wedge}}$, $\mathbf{CB^{\wedge-}}$, and $\mathbf{CB^{\wedge 2-}}$ the contributions of the respective forms of quinoidal bases, hemiketals, and *cis*-chalcones. For example, the mole fraction distribution of $\mathbf{CB^{-\wedge}}$ is given by eq. (27) (Mendoza et al. 2019 supplementary information).

$$X_{CB-\wedge} = X_{A-} + X_{B-} + X_{Cc-} = a_1 \frac{K_a^{\wedge} K_a^{\wedge\wedge} \left[H^+\right]}{D^{\wedge}} + b_1 \frac{K_a^{\wedge} K_a^{\wedge\wedge} \left[H^+\right]}{D^{\wedge}} + c_1 \frac{K_a^{\wedge} K_a^{\wedge\wedge} \left[H^+\right]}{D^{\wedge}} \quad (27)$$

with

$$D^{\wedge} = \left[H^+\right]^3 + K_a^{\wedge} \left[H^+\right]^2 + K_a^{\wedge} K_a^{\wedge\wedge} \left[H^+\right] + K_a^{\wedge} K_a^{\wedge\wedge} K_a^{\wedge\wedge\wedge} \quad (28)$$

and

$$a_1 + b_1 + c_1 = 1 \quad (29)$$

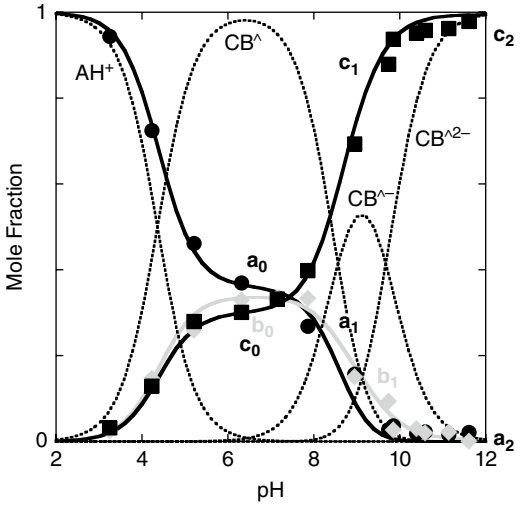

Figure 1.4 Representation of the mole fraction distribution of the compound 4'-hydroxyflavylium on the basis that the reverse pH jumps at pseudo-equilibrium. The symbol ^ is used to differentiate pseudo-equilibrium from equilibrium (').

The mole fractions of the more colored forms, eq. (30), as well of those of hemiketals, eq. (31) and *cis*-chalcones, eq. (31) are thus obtained.

$$X_{AH+} + X_A + X_{A-} + X_{A2-} = \frac{\left[H^+\right]^3 + a_0 K_a^{\wedge}\left[H^+\right]^2 + a_1 K_a^{\wedge} K_a^{\wedge\wedge}\left[H^+\right] + a_2 K_a^{\wedge} K_a^{\wedge\wedge} K_a^{\wedge\wedge\wedge}}{D^{\wedge}} \quad (30)$$

$$X_B + X_{B-} + X_{B2-} = \frac{b_0 K_a^{\wedge}\left[H^+\right]^2 + b_1 K_a^{\wedge} K_a^{\wedge\wedge}\left[H^+\right] + b_2 K_a^{\wedge} K_a^{\wedge\wedge} K_a^{\wedge\wedge\wedge}}{D^{\wedge}} \quad (31)$$

$$X_{Cc} + X_{Cc-} + X_{Cc2-} = \frac{c_0 K_a^{\wedge}\left[H^+\right]^2 + c_1 K_a^{\wedge} K_a^{\wedge\wedge}\left[H^+\right] + c_2 K_a^{\wedge} K_a^{\wedge\wedge} K_a^{\wedge\wedge\wedge}}{D^{\wedge}} \quad (32)$$

Considering that the apparent equilibrium constants are experimentally obtained from the inflection points of the absorption spectra as a function of pH, the fitting of eq. (30) to eq. (32) permits us to obtain the constants a_n, b_n and c_n (n = 0, 1 and 2).

On the other hand, eq. (22) to eq. (25) can be re-written for the pseudo-equilibrium:

$$X_{AH+} + X_A + X_{A-} + X_{A2-} = \frac{\left[H^+\right]^3 + K_a\left[H^+\right]^2 + K_{A/A-}K_a\left[H^+\right] + K_{A-/A2-}K_{A/A-}K_a}{D^{\wedge}} \quad (33)$$

$$X_B + X_{B-} + X_{B2-} = \frac{K_h\left[H^+\right]^2 + K_{B/B-}K_h\left[H^+\right] + K_{B-/B2-}K_{B/B-}K_h}{D^{\wedge}} \quad (34)$$

$$X_{Cc} + X_{Cc-} + X_{Cc2-} = \frac{K_h K_t\left[H^+\right]^2 + K_{Cc/Cc-}K_h K_t\left[H^+\right] + K_{Cc-/Cc2-}K_{Cc/Cc-}K_h K_t}{D^{\wedge}} \quad (35)$$

Comparing eq. (30) with eq. (33), eq. (31) with eq. (34), and eq. (32) with eq. (35) the following relations are obtained:

$$K_a = a_0 K_a^{\wedge};\ K_h = b_0 K_a^{\wedge};\ K_t = \frac{c_0 K_a^{\wedge}}{K_h} \quad (36)$$

$$K_{A/A-} = \frac{a_1 K_a^{\wedge} K_a^{\wedge\wedge}}{K_a};\ K_{B/B-} = \frac{b_1 K_a^{\wedge} K_a^{\wedge\wedge}}{K_h};\ K_{Cc/Cc-} = \frac{c_1 K_a^{\wedge} K_a^{\wedge\wedge}}{K_h K_t} \quad (37)$$

$$K_{A-/A2-} = \frac{a_2 K_a^{\wedge} K_a^{\wedge\wedge} K_a^{\wedge\wedge\wedge}}{K_{A/A-}K_a};\ K_{B-/B2-} = \frac{b_2 K_a^{\wedge} K_a^{\wedge\wedge} K_a^{\wedge\wedge\wedge}}{K_{B/B-}K_h};\ K_{Cc-/Cc2-} = \frac{c_2 K_a^{\wedge} K_a^{\wedge\wedge} K_a^{\wedge\wedge\wedge}}{K_{Cc/Cc-}K_h K_t} \quad (38)$$

1.3.2 Reverse pH Jumps from Equilibrium

From eq. (36) to eq. (38) all equilibrium constants except those regarding the *trans*-chalcones can be obtained. Moreover, the *cis-trans* isomerization constants can be calculated

from a reverse pH jump from the equilibrated solutions. Considering that formation of the flavylium cation from the *trans*-chalcones is very slow, this kinetics should be followed by a standard spectrophotometer. The quinoidal bases, hemiketals, and *cis*-chalcones are transformed to flavylium cation much faster than the *trans*-chalcones and appear as an initial absorption.[2] From this point all the equilibrium constants have been calculated. The mole fraction of *trans*-chalcone is thus obtained from the ratio of the absorbance of the trace amplitude/total absorbance. The mole fractions of the other species at equilibrium are obtained from those at pseudo-equilibrium, calculating the respective proportion.[3] For example, if at pseudo-equilibrium **A**=0.3, **B**=0.2, and **Cc**=0.5 and the mole fraction of **Ct** at equilibrium is 0.5, the mole fractions of **A**, **B**, and **Cc** at equilibrium are the following: **A**=0.15, **B**=0.1, and **Cc**=0.25.

1.4 The Kinetic Processes

Scheme 1.5 represents the four kinetic processes of anthocyanins and related compounds in acidic medium. It is worth noting that, like in the case of the formation of the quinoidal base from flavylium cation, all the other anionic species are formed as in Scheme 1.3, from proton transfer. This reaction represents step 1 in the kinetic process and takes place in microseconds during the mixing time of the stopped flow. Only using special techniques

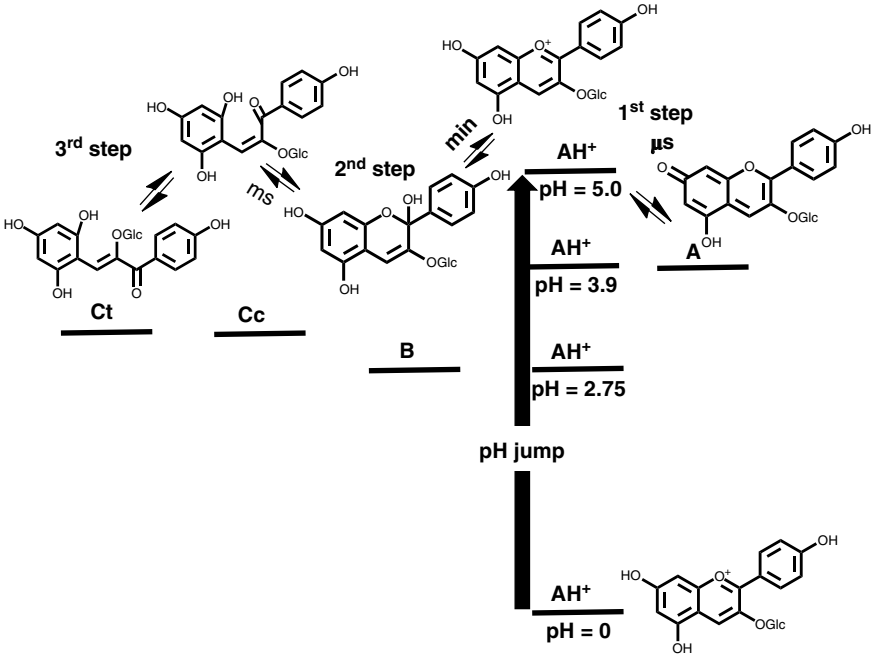

Scheme 1.5 Energy level diagram of the relative thermodynamic level of the five species of pelargonidin-3-glucoside appearing in acid medium. The three distinct kinetic steps taking place in very different time scales are observed, allowing for separation of the kinetics into three kinetic equations.

such as temperature jumps (Brouillard and Dubois 1977), and in some favourable cases flash photolysis, are these constants obtained.[4] This fact makes the kinetics reported in Scheme 1.5 the only relevant ones upon direct pH jumps, since the formation of the anionic species is immediate when compared with hydration, tautomerization, and isomerization. Moreover, the first process after a direct pH jump (from flavylium cation) is the formation of the quinoidal base, which equilibrates with the flavylium cation. In the subsequent kinetic steps these two species behave as a single one.

The following kinetic step is the hydration followed by tautomerization (Scheme 1.5). Except in very acidic solutions (not accessed by direct pH jumps), the tautomerization reaction is faster than hydration and by consequence this last one is the rate-determining step of this kinetic process. This kinetic step can thus be considered as in eq. (39).

During the hydration both **AH$^+$**/**A** and **B**/**Cc** can be considered as a single species.

$$k_2 = X_{AH^+}k_h + X_{Cc}k_{-h}\left[H^+\right] = \frac{\left[H^+\right]}{\left[H^+\right]+K_a} + \frac{1}{1+K_t}k_{-h}\left[H^+\right] \tag{39}$$

where X_{AH+} is the mole fraction of **AH$^+$** in its equilibrium with **A**, and X_B is the mole fraction of **A** in its equilibrium with **Cc**.

In eq. (39) the forward reaction takes place only from the reaction of **AH$^+$** to form **B**, because, as mentioned above, the quinoidal base **A** does not hydrate in acidic medium (Brouillard and Dubois 1977).

For anthocyanins and many of the flavylium derivatives, the last step is controlled by the isomerization of chalcones, which is by far the slowest process of the kinetics. A similar reasoning used for step 2 can be made for step 3. In this case all species except **Ct** can be considered equilibrated.

$$k_3 = X_{Cc}k_i + k_{-i} = \frac{K_hK_t}{\left[H^+\right]+\hat{K_a}}k_i + k_{-i} \tag{40}$$

1.4.1 Heavenly Blue Anthocyanin

The experimental procedure above reported was used to rationalize the multistate of heavenly blue anthocyanin and two derivatives (Scheme 1.6).

Heavenly blue anthocyanin, HBA1, has attracted the attention of the scientific community due to its peculiar properties, specifically the fact that the same anthocyanin is used by the plant to confer purplish color to the buds and blue color to the petals (Yoshida et al. 1995; Goto and Kondo 1991; Kondo et al. 1992). Moreover, *in vitro* the blue color is persistent in neutral and moderately basic solutions (Kondo et al. 1992; Yoshida et al. 2009). Structural information regarding HBA1 fully supports the intramolecular stacking shown in Scheme 1.7.

The system was studied up to the mono-anionic forms because at higher pH values a slow decomposition takes place and the data does not have sufficient accuracy. In spite of equilibrium being reached in one to two weeks, the neutral and mono-anionic species are relatively stable. Table 1.1 summarizes the data.

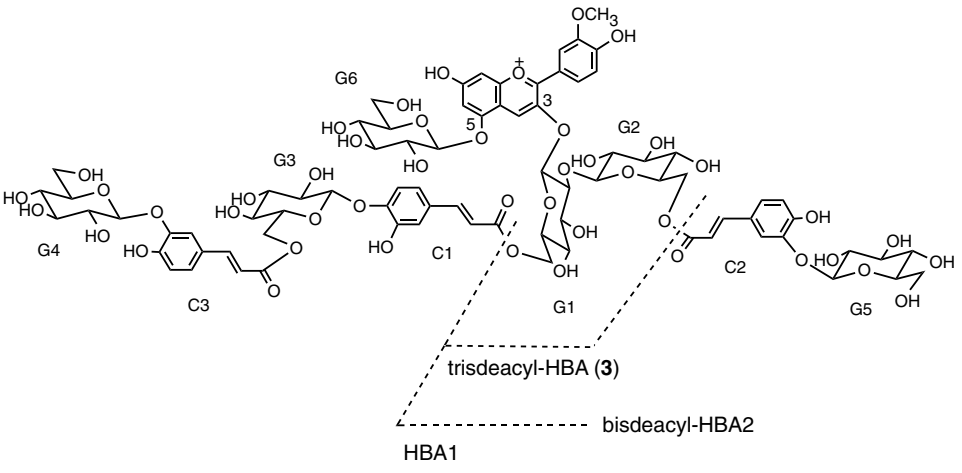

Scheme 1.6 Heavenly blue anthocyanin HBA1 and their derivatives bis-deacyl-HBA2 and tris-deacyl-HBA3. *Source:* Mendoza et al. 2018.

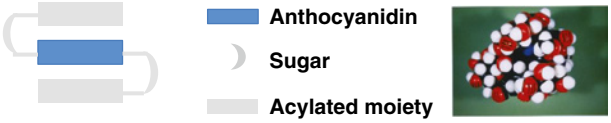

Scheme 1.7 Sketch representing the intramolecular copigmentation in polyacylated anthocyanins; CPK models of heavenly blue anthocyanin. *Source:* Mendoza et al. 2018.

Table 1.1 Equilibrium constants of heavenly blue anthocyanin and their derivatives.

	pK'_a	pK''_a	$pK\hat{}_a$	p_{Ka}	pK_h	K_t
HBA1	3.5	7.3	3.6	3.8	4.6	1.1
HBA2	—	—	2.92	4.23	3.1	0.35
HBA3	—	—	1.95	4.19	2.1	0.37
	K_i	$pK\hat{}\hat{}_a$	pK_{A/A^-}	pK_{B/B^-}	pK_{Cc/Cc^-}	pK_{Ct/Ct^-}
HBA1	4.0	7.35	7.35	7.5	7.25	7.36

Estimated error 10%.

Source: Mendoza et al. 2018

In Table 1.1 the equilibrium constants of the non-acylated, di-acylated and tri-acylated derivatives of heavenly blue anthocyanin are also reported (Scheme 1.8). HBA2 and HBA3 behave as common anthocyanins, being relatively stable only in acidic medium, preventing the calculation of the data regarding the anionic species at equilibrium.

The mole fraction distribution for HBA1 of the several species is represented in Figure 1.5. This distribution is in line with the previous observation (Yoshida et al. 1995) that the buds of heavenly blue anthocyanin are purple while the petals are blue. In fact the pH of the vacuoles in buds is around 6.6, while in petals pH=7.7 (Yoshida et al. 1995). In that pH